Polymerase III transcription is necessary for T cell priming by dendritic cells

Marisa Reverendo, Rafael J Argüello, Christine Polte, Jan Valečka, Voahirana Camosseto, Nathalie Auphan-Anezin, Zoya Ignatova, Evelina Gatti, Philippe Pierre

Polymerase III transcription is necessary for T cell priming by dendritic cells

Marisa Reverendo[a,b,c], Rafael J. Argüello[a], Christine Polte[d], Jan Valečka[a], Voahirana Camosseto[a,c], Nathalie Auphan-Anezin[a], Zoya Ignatova[d], Evelina Gatti[a,b,c,e,1,2], and Philippe Pierre[a,b,c,e,1,2]

[a]Aix Marseille Université, CNRS, INSERM, Centre d'Immunologie de Marseille-Luminy (CIML), 13288 Marseille Cedex 9, France; [b]Institute for Research in Biomedicine, Department of Medical Sciences, University of Aveiro, 3810-193 Aveiro, Portugal; [c]CNRS "Mistra," International Associated Laboratory, 13288 Marseille Cedex 9, France; [d]Institute for Biochemistry and Molecular Biology, University of Hamburg, 21046 Hamburg, Germany; and [e]Ilidio Pinho Foundation, 4150–146 Porto, Portugal

Edited by Hidde L. Ploegh, Boston Children's Hospital, Boston, MA, and approved September 27, 2019 (received for review March 13, 2019)

Exposure to microbe-associated molecular patterns (MAMPs) causes dendritic cells (DCs) to undergo a remarkable activation process characterized by changes in key biochemical mechanisms. These enhance antigen processing and presentation, as well as strengthen DC capacity to stimulate naïve T cell proliferation. Here, we show that in response to the MAMPS lipopolysaccharide and polyriboinosinic:polyribocytidylic acid (Poly I:C), RNA polymerase III (Pol III)-dependent transcription and consequently tRNA gene expression are strongly induced in DCs. This is in part caused by the phosphorylation and nuclear export of MAF1 homolog negative regulator of Poll III (MAF1), via a synergistic casein kinase 2 (CK2)- and mammalian target of rapamycin-dependent signaling cascade downstream of Toll-like receptors (TLRs). De novo tRNA expression is necessary to augment protein synthesis and compensate for tRNA degradation driven by TLR-dependent DC exposure to type-I IFN. Although protein synthesis is not strongly inhibited in absence of RNA Pol III activity, it compromises the translation of key DC mRNAs, like those coding for costimulatory molecules and proinflammatory cytokines, which instead can be stored in stress granules, as shown for CD86 mRNA. TLR-dependent CK2 stimulation and subsequent RNA Pol III activation are therefore key for the acquisition by DCs of their unique T cell immunestimulatory functions.

casein kinase 2 | interferon | protein synthesis | CD86 | immunity

Dendritic cells (DCs) are key regulators of both protective immune responses and tolerance to self-antigens (1). DCs are professional antigen presenting cells (APCs), equipped with pattern recognition receptors, like Toll-like receptors (TLRs), capable of recognizing and responding to microbe-associated molecular patterns (MAMPs) (2). For example, lipopolysaccharide (LPS) detection by TLR4 promotes DC activation by triggering a series of signaling cascades resulting in massive changes in gene expression, membrane traffic, and metabolism. This maturation process ultimately culminates in the priming of naïve T cell recognizing antigenic peptides presented by major histocompatibility complexes (MHCs) and costimulatory molecules at the surface of activated DCs (3, 4). LPS-stimulated DCs undergo a phase of rapid up-regulation of protein synthesis mediated in part through the mammalian target of rapamycin (mTORC1) signal transduction pathway. This up-regulation is necessary for cytokine production and rapid increase in surface MHC class II and costimulatory molecules, like B7.1/CD86 (5). Importantly the secretion of type-I IFN (IFN) contributes majorly to the speed and intensity of DC maturation in an autocrine manner (6). The role of RNA polymerase III (Pol III) activity and tRNA gene expression during DC activation has remained unexplored. Pol III is responsible for the transcription of some 300 different genes (class III genes), that are mostly tRNAs (7). In-depth analysis of Pol III activity has revealed a cascade of coordinated interactions of transcription factors to recruit Pol III and allow the transcription of tRNA genes. TFIIIC binding to intragenic conserved promoters is followed by assembly of initiation factor TFIIIB subunits (Brf1, Bdp1, and TBP) and binding to upstream sequences, that lead to the subsequent recruitment of the Pol III subunits (8–10). Pol III is normally controlled by the general negative regulator MAF1 (11), which binds to the polymerase and impairs its recruitment to the promoter DNA/TFIIB complex, and thus prevents transcription initiation.

We show here that TLR agonists drive up global tRNA transcription during the first hours of DC activation. Following LPS stimulation, enhanced Pol III transcription is achieved through the concerted actions of casein kinase 2 (CK2) and mTORC1 on the MAF1 repressor. TLR-dependent nuclear translocation of both CK2 and mTORC1 causes MAF1 phosphorylation and cytosolic accumulation over time, consequently allowing for Pol III transcriptional activation. This cascade of signaling events enhancing tRNAs expression is necessary to increase protein synthesis and harness DCs with the full immunestimulatory potential required for priming naïve T cells. We also found that DC exposure to type-I IFN accelerates tRNA turnover. Enhanced Pol III transcription upon TLR triggering is therefore necessary to compensate for IFN-dependent tRNA decay, which would, in absence of this mechanism, drive the formation of stress granules (SGs) and prevent the translation of key mRNAs, such as *CD86*, in activated DCs. These SGs differ from the SGs formed by environmental stress, since they are independent of full protein synthesis inhibition and increased eukaryotic translation initiation factor 2 alpha subunit (eIF2α) phosphorylation, 2 hallmarks of SGs formed in response to oxidative stress (12). The CK2/MAF1/Pol III axis represents therefore a previously unidentified signaling

Significance

RNA polymerase III-dependent transcription and increased tRNA expression are necessary for MAMP-stimulated DCs to stimulate naïve T cells. Augmented Pol III-dependent transcription is as essential as the switch to glycolysis and other energetic metabolism variations that are now considered as hallmarks of immune cell activation and are all necessary to increase protein synthesis in these cells.

Author contributions: M.R., R.J.A., N.A.-A., Z.I., and P.P. designed research; M.R., R.J.A., C.P., V.C., N.A.-A., and Z.I. performed research; C.P. contributed new reagents/analytic tools; M.R., R.J.A., C.P., J.V., Z.I., E.G., and P.P. analyzed data; and M.R., Z.I., E.G., and P.P. wrote the paper.

The authors declare no competing interest.

This article is a PNAS Direct Submission.

[1]E.G. and P.P. contributed equally to this work.

[2]To whom correspondence may be addressed. Email: gatti@ciml.univ-mrs.fr or pierre@ciml.univ-mrs.fr.

This article contains supporting information online at www.pnas.org/lookup/suppl/doi:10.1073/pnas.1904396116/-/DCSupplemental.

cascade downstream of TLRs, that is essential for naïve T cell priming by DCs.

Materials and Methods

Cell Culture. Bone marrow (BM)-derived DCs were differentiated in vitro from 6- to 8-wk-old female mice bone marrow with granulocyte macrophage colony-stimulating factor (GM-CSF) (13). Mouse splenocytes were obtained by dissociation of spleens using Liberase TL, followed by a 25-min incubation at 37 °C. Cells were washed (1× PBS + 2% FBS [FCS] + 2 mM EDTA) and passed in a 70-mm cell strainer and centrifuged for 5 min at 4 °C. DCs were purified using CD11c Positive Selection Kit from Milteny (CD11c MicroBeads UltraPure) according to manufacturer's instructions for prior culture in RPMI and 10% FCS. All experiments were approved by the Comité d'Éthique de Marseille and the Direction Départementale des Services Vétérinaires des Bouches du Rhône (approval no. A13-543).

Flow Cytometry. Cell were harvested and washed with PBS, incubated with the antibody mixture diluted in cold fluorescence-activated cell sorting (FACS) buffer for 30 min at 4 °C. Intracellular staining was performed after fixation with Cytofix/Cytoperm (BD Biosciences), by incubation with antibody mixture diluted in PermWash (BD Biosciences). Samples were acquired on a FACS Canto II and analyzed with FlowJo (Tree Star). Antibodies used were CD11c (N418) and CD86 (GL-1) from BioLegend and MHCII (M5/114.15.2) from eBioscience. For the spleen cells, the antibodies were CD11c (N418), CD8α (53-6.7), and MHCII (M5/114.15.2) from eBioscience; BST2 (927), CD86 (GL-1), and SiglecH (551) from BioLegend; and CD11b (M1/70) and B220 (RA3-6B2) from BD Biosciences.

Immunoblotting. Cell pellets were extracted with radioimmunoprecipitation assay (RIPA) buffer supplemented with complete protease and phosphatase inhibitor mixture tablets (Roche). Protein quantification was done with the bicinchoninic acid (BCA) protein assay (Pierce). A total of 20 to 25 μg of sample was run in SDS–polyacrylamide gels and Phos-Tag polyacrylamide gels. Antibodies against eIF2α, p-eEF2(Thr56), eEF2, p-AKT, AKT, and p-p65 were from Cell Signaling. Antibody against p-eIF2α(S51) was from ABCAM; antibody against β-actin was from Sigma. Mouse antibody against puromycin (25D1) was purchased from Merck Millipore. Antibody against p-eIF2β was a kind gift from David Litchfield, University of Western Ontario, London, ON, Canada. Antibody against eIF2β and p-65 was purchased from Santa Cruz Biotechnology. HRP secondary antibodies were from Jackson ImmunoResearch Laboratories.

Northern Blot. Northern blots were performed as previously described (14). In short, total RNA was extracted using TRIzol (Invitrogen) and resolved on 15% polyacrylamide gels and transferred to a nitrocellulose membrane (Hybond N, Amersham) that was crosslinked using a UV Stratalinker 1800 (Stratagene). Membranes were hybridized overnight at the melting temperature (Tm) of the nucleotides lowered by 5 °C, then scanned and analyzed using ImageJ.

ELISA. Mouse IL-6 and TNF-α were quantified using an appropriate ELISA kit (eBioscience) according to the manufacturer's instructions.

Further detailed methods are provided in *SI Appendix*.

Results

tRNAs Are Up-Regulated during DC Activation by MAMPs. We used microarrays capturing all tRNA isoacceptors (15, 16) to monitor globally their expression in LPS-activated bone marrow-derived DCs (bmDCs). tRNA levels were quantified after 4 h and 8 h of LPS activation in WT and IFN receptor-deficient ($IFNAR^{-/-}$) bmDCs (Fig. 1*A* and *SI Appendix*, Tables S2 and S3). $IFNAR^{-/-}$ cells display a delayed response to LPS, caused by their incapacity to sense autocrine type-I IFN, a key potentiator of their activation (6). LPS stimulation up-regulated most tRNA isoacceptors after 4 h, followed by a return to preactivation levels after 8 h (Fig. 1*A*). In $IFNAR^{-/-}$ DCs, tRNA expression remained nearly unchanged in the first hours of LPS activation, whereas up-regulation was observed after 8 h of stimulation. The expression of several tRNAs (e.g., Arg-CCU, Lys-UUU1, Gln-C/UUU, Ala-A/C/UGC, Ile-IAU, Leu-A/UAG, Leu-CAG, and Leu-UAA2) was even augmented compared to the levels found in 4-h LPS-stimulated WT cells (*SI Appendix*, Tables S2 and S3). These variations likely reflect the key contribution of type-I IFN to DC maturation (*SI Appendix*, Fig. S1) (6), but also suggest that DC activation by type-I IFN could impact the stability or turnover of tRNAs.

To extend our analysis to physiologically relevant DC types and stimuli, we performed qPCR and Northern blot to monitor $tRNA^{Tyr}$ (GUA), $tRNA^{Thr}$ (AGU), and $tRNA^{Arg}$ (UCU) expression in activated bmDCs (Fig. 1 *B* and *C*) or $CD11C^{+}$ splenic DCs (Fig. 1*D*). The TLR3 agonist Poly I:C was chosen next to TLR4-dependent stimulation with LPS, because Poly I:C promotes mostly type-I IFN production in DCs and drives a slower kinetics of activation (13). tRNA expression was found to be augmented by 2- to 3-fold after 8 h of stimulation with Poly I:C. Activated $IFNAR^{-/-}$ bmDCs displayed little induction of these tRNAs compared to their WT counterparts (Fig. 1*B*). The latter result was confirmed by Northern blot for $tRNA^{Tyr}$ (GUA) expression, which increased in response to both MAMPs (Fig. 1*C*), but not in absence of IFNAR. Increased $tRNA^{Tyr}$ expression was also observed in primary splenic DCs (Fig. 1*D*), further demonstrating the general relevance of these observations. Importantly, $tRNA^{Tyr}$ was unchanged following treatment with the RNA Pol III inhibitor ML-60218 (17) (Fig. 1*E*), suggesting that RNA Pol III activity and de novo tRNA transcription is involved in DC maturation. Increased $tRNA^{Tyr}$ expression was paralleled by an up-regulation of the RNA polymerase III subunit C mRNA (*Polr3C*) (Fig. 1*F*), potentially contributing to the increased tRNA transcription in activated DCs. Importantly, RNA Pol III has been described as a sensor for viral DNA (18), and the lack of *Polr3C* mRNA induction in activated $IFNAR^{-/-}$ DCs (Fig. 1*F*) suggests that *Polr3C*, like many cytosolic nucleic acid sensors, behaves as an IFN-stimulated gene (ISG).

To gain a better understanding of tRNA homeostasis with respect to IFNAR signaling, we investigated the turnover of $tRNA^{Tyr}$ (GUA) following treatment with LPS and RNA Pol III inhibitor by Northern blot (Fig. 1*G*) and qPCR (Fig. 1*H*). Although tRNAs are believed to be stable and long lived in most cells (19), we found that 30 to 50% of $tRNA^{Tyr}$ (GUA) were degraded in DCs after 7 h of LPS activation, in absence of active Pol III transcription. This decay did not occur upon IFNAR deletion (Fig. 1 *G* and *H*), indicating that type-I IFN detection compromises tRNA stability and that enhanced Pol III transcription is required to maintain sufficient tRNA levels to sustain active protein synthesis during DC activation.

RNA Pol III Activity Is Required for DC Activation. Pol III inhibition with ML-60218 did not affect protein synthesis in nonactivated DCs, but efficiently prevented its augmentation triggered by LPS or Poly I:C, as monitored by puromycin incorporation (Fig. 2*A*). A similar observation was made upon treatment with 2-deoxy-glucose (2-DG) (Fig. 2*B*), that inhibits the glycolytic shift required for full DC activation (20, 21) and serves here as a pharmacological control.

Given the inhibitory activity of ML-60218 on the protein synthesis up-regulation normally driven by LPS stimulation, we explored the consequences of inhibiting Poll III on the translation machinery organization in activated DCs. We monitored by confocal microscopy the formation of stress granules in different conditions (Fig. 2*C*) (12). SGs form in the cytoplasm of cells exposed to acute stress (e.g., oxidative stress) concomitantly with eIF2α phosphorylation and global inhibition of the protein synthesis. SGs store mRNAs mostly stalled at initiation in complexes with 40S ribosomal subunits, P-eIF2α and RNA-binding proteins, e.g., G3BP-stress granule assembly factor 1 (G3BP1). SGs are located in the vicinity of other RNA–protein organelles, the P bodies that concentrate the mRNA decay machinery, such as the decapping mRNA 1A enzyme (DCP1A) and participate in RNA turnover through constant exchanges with SGs (12, 22). Enhanced SG formation was observed in control DCs treated with arsenite (Ars, 30 min), monitored by the G3PB1 SG marker (Fig. 2*C*). A moderate increase in SG formation was also detected in

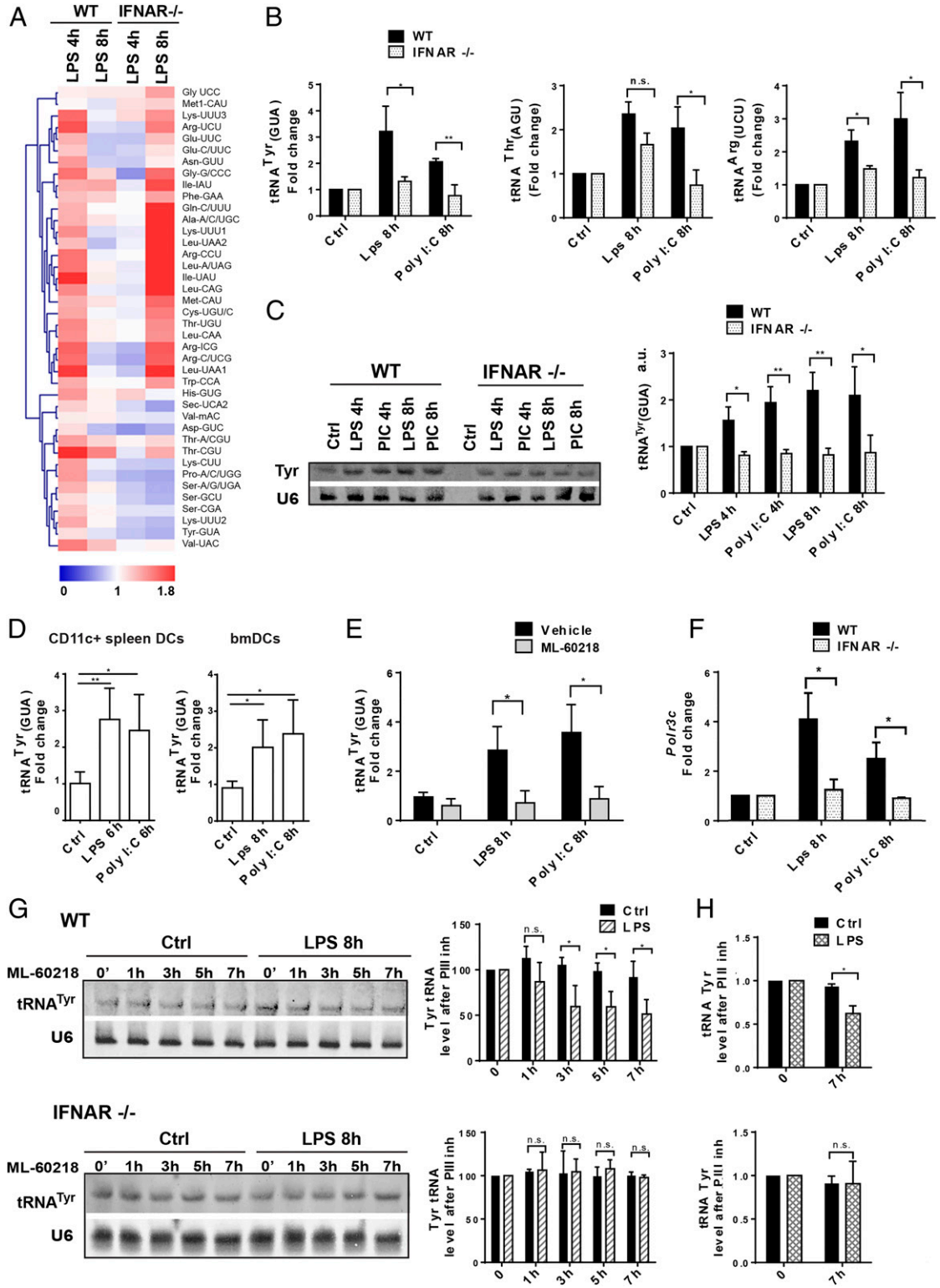

Fig. 1. Alterations of tRNA transcription following DC activation by MAMPs. (*A*) Heatmap of tRNA expression levels measured by tRNA-tailored microarrays of WT and IFNAR$^{-/-}$ DCs stimulated with LPS for 4 and 8 h. Data ($n = 2$) are relative to the expression levels at time point zero. tRNAs are presented by their cognate amino acid and anticodon. Meti-CAU and Met-CAU are initiator and elongator tRNAMet (CAU), respectively. (*B*) tRNA^{Tyr} (GUA), tRNA^{Thr} (AGU), and tRNA^{Arg} (UCU) levels measured by RT-qPCR in WT and IFNAR$^{-/-}$ DCs stimulated with LPS or Poly I:C for 4 and 8 h. (*C*) tRNA^{Tyr} (GUA) levels measured by Northern blot in WT and IFNAR$^{-/-}$ DCs; densitometry quantifications are shown (*Right*). (*D*) tRNA^{Tyr} (GUA) levels measured by RT-qPCR in bmDCs and CD11c^{+} spleen DCs. (*E*) tRNA^{Tyr} (GUA) levels measured in LPS or Poly I:C-activated DCs, treated with the Pol III inhibitor ML-60218 by RT-qPCR. (*F*) *Polr3c* mRNA levels measured by RT-qPCR in WT and IFNAR$^{-/-}$ DCs. (*G*) Northern blot analysis of tRNA^{Tyr} (GUA) decay in LPS-activated WT and IFNAR$^{-/-}$ DCs treated with ML-60218 for indicated time; densitometry quantification is shown (*Right*). (*H*) Decay of tRNA^{Tyr} (GUA) analyzed by RT-qPCR in WT and IFNAR$^{-/-}$ DCs after 7 h of LPS and ML-60218 treatment. Data in *B*–*H* are mean ± SD ($n = 3$). n.s., nonsignificant results; $^{*}P < 0.05$, $^{**}P < 0.01$ by unpaired Student's *t* test.

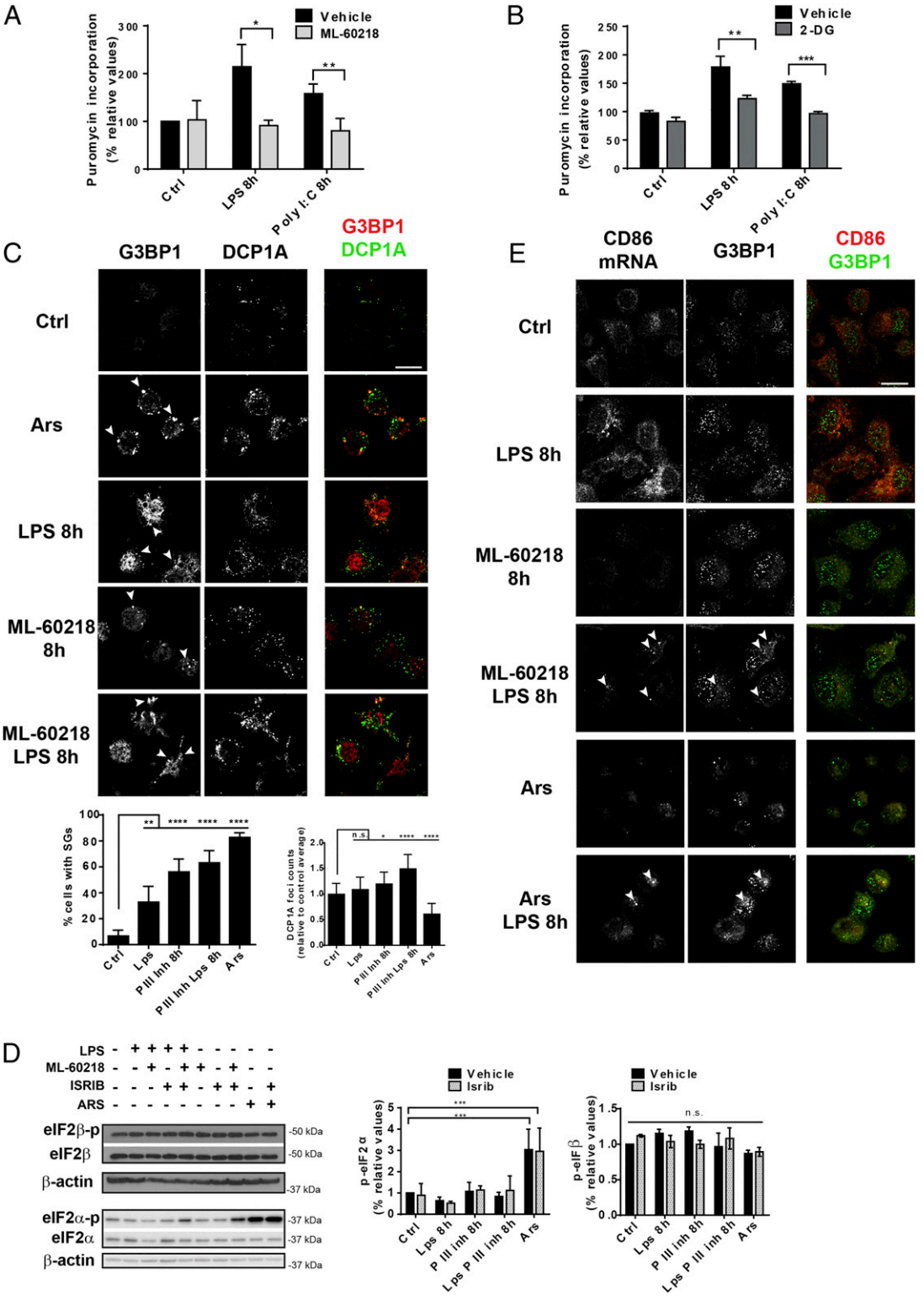

Fig. 2. Pol III activity contributes to DC activation. (*A*) Protein synthesis was measured by flow cytometry using puromycin incorporation in LPS- or Poly I:C-stimulated DCs treated or not with ML-60218 for 8 h or (*B*) with 2-DG. (*C*) Immunofluorescence microscopy for G3BP1 and DCP1A in Ars-treated (30 min) or LPS-activated DCs treated with or without ML-60218. SG and DCP1A foci quantification is shown at the *Bottom*. Arsenite-treated cells were used as positive control. G3BP1-positive SGs are indicated by arrowheads. (Scale bar, 10 μm.) Quantification of G3BP1- and DCP1A-positive granules is shown at the *Bottom*. (*D*) Levels of phosphorylated and total eIF2α and eIF2β monitored by immunoblot. (*E*) In situ hybridization fluorescence staining for CD86 mRNA, along with SG marker (G3BP1) in LPS-stimulated DCs treated or not with ML-60218. Arsenite treatment was used as positive reference. CD86 mRNA localized in SG is indicated by arrowheads. (Scale bar, 10 μm.) All images are representative of $n = 3$ independent experiments. Data in *A*–*D* are mean ± SD ($n = 3$). (*A* and *B*) $^{*}P < 0.05$, $^{**}P < 0.01$, $^{***}P < 0.001$ by unpaired Student's *t* test. Data in *C* and *D* are mean ± SD ($n = 3$), n.s., nonsignificant results; $^{**}P < 0.01$ and $^{****}P < 0.0001$ with multiple comparison with Holm–Sidak correction.

LPS-activated DCs. However, treatment with ML-60218 alone or in combination with LPS caused even higher formation of SGs and P bodies/DCP1A foci (Fig. 2*C*). Surprisingly, and unlike SGs assembling upon oxidative stress, ML-60218–dependent foci formed independently of eIF2α phosphorylation, which like phosphorylated eIF2β remained unaffected by ML-60218 (Fig. 2*D*). These granules were insensitive to the integrated stress response inhibitor (ISRIB) (Fig. 2*D* and *SI Appendix*, Fig. S2), a small inhibitor of the integrated stress response interfering with SGs (23). This suggests the existence of an alternative pathway governing SGs upon depletion of tRNAs and other Pol III-dependent transcripts (24), which facilitates SG formation without heavy eIF2α phosphorylation and full protein synthesis inhibition, as opposed to what is observed upon Ars treatment (Fig. 2*D*) (12). These SGs sequester mRNAs encoding activated DC transcripts, like the costimulatory receptor CD86 mRNA, which associated with G3BP1 in both ML-60218 or Ars treatment (Fig. 2*E*). mRNA segregation in SGs likely prevents their translation, inferring that enhanced Pol III transcription by TLR agonists is a crucial function that controls protein synthesis, both quantitatively and probably qualitatively, during DC functional activation.

Casein Kinase 2 Controls Pol III Activation. Pol III-mediated transcription is inhibited via a mechanism that depends on the nuclear accumulation of the MAF1 repressor, followed by its physical association with the polymerase (25). In yeast, phosphorylation of MAF1 by casein kinase II (CK2) is required for efficient Pol III transcription (26). We monitored MAF1 phosphorylation levels by Phos-Tag immunoblots and found them to be strongly enhanced following DC stimulation both with LPS and Poly I:C (Fig. 3*A*). Increased P-MAF1 levels were associated with its export out of the nucleus, as visualized by confocal microscopy in LPS-stimulated cells (*SI Appendix*, Fig. S3). We next investigated the consequences of MAF1 activity on tRNA transcription by silencing its expression or overexpressing it ectopically. Abrogation of *Maf1* expression by RNAi strongly augmented $tRNA^{Tyr}$ expression in steady-state DCs to levels observed in the activated cells (Fig. 3 *B*, *Left*). Conversely, MAF1 overexpression prevented up-regulation of $tRNA^{Tyr}$ upon LPS stimulation (Fig. 3 *B*, *Right*). Our results suggest that MAF1 is a key transcription factor controlling tRNA transcription during DC activation.

The involvement of CK2 in this process was tested using CX-4945, a specific inhibitor currently used in clinical trials (27, 28). Immunoblotting for different targets of CK2 (AKT and eIF2β) was performed to confirm CX-4945's specificity in DCs (Fig. 3*C*). AKT and eIF2β phosphorylation was completely abolished following CX-4945 treatment, demonstrating its efficacy in vitro. CX-4945 also prevented P-MAF1 accumulation in both steady-state and activated DCs (Fig. 3*D*) and inhibited its nuclear export in response to LPS (*SI Appendix*, Fig. S3). As anticipated from the inhibition of Pol III activity by MAF1, TLR-dependent enhancement of $tRNA^{Tyr}$ (GUA) transcription was completely abrogated by CX-4945 (Fig. 3*D*). This confirms that CK2 activity controls Pol III through MAF1 phosphorylation upon TLR stimulation. Treatment with rapamycin, a potent mTOR inhibitor, had the same effects (*SI Appendix*, Fig. S4), suggesting that both CK2 and mTORC1 act together to control Pol III transcription during DC activation. MAF1 phosphorylation has to be efficient to fully unleash Pol III transcription. Immunoproximity ligation assay (iPLA) showed that upon stimulation with LPS, CK2 can be found in the nucleus, in close vicinity of the BRF1 subunit of TFIIIB, that recruits Pol III on tRNA promotors together with MAF1 (Fig. 4*A*). During activation, MAF1/CK2 (Fig. 4*B*) or MAF1/MTOR (*SI Appendix*, Fig. S4*D*) complexes were mostly found in the cytosol (1.5 h), before accumulating in nuclei of activated cells at later times (3 or 6 h). This confirms that TLR signaling causes both CK2 and mTORC1 migration into the nucleus to promote MAF1 export and potentiate Pol III activation, contributing to enhanced protein synthesis and acquisition of their immune-stimulatory function by DCs. The inhibitory effect of CX-4945 on tRNA expression and protein synthesis was confirmed by the formation of SGs in treated control or LPS-activated DCs (Fig. 4*C*), further suggesting that CK2 activity is also required in steady-state DCs to promote Pol III activity and basal tRNA transcription.

CK2 and Pol III Are Required for T Cell Priming by DCs. DCs treated with CX-4945 were deficient in their activation, as demonstrated by the lack of up-regulation of surface CD86 and MHCII in response to LPS and Poly I:C (Fig. 5*A*). We also demonstrate that CK2 inhibition by CX-4945, in addition to blocking phosphorylation of AKT and the ribosomal protein S6, also strongly prevented NF-κB p65 phosphorylation (Fig. 5*B*) (29). This likely interferes with DC activation and proinflammatory cytokine production, providing direct evidence of the capacity of CK2 to control signal transduction downstream of TLRs. Inhibition of the NF-κB signaling pathway is probably the dominant feature of CX-4945, that synergizes with the reduction in tRNA expression to prevent DC activation. To unravel the singular impact of inhibiting Pol III transcription on DC immunological function, we monitored by flow cytometry the surface expression of costimulatory molecules after DC stimulation in presence of ML-60218. Similarly to glycolysis inhibition by 2-DG treatment, used as a positive control, surface CD86 and CD40 expression was strongly reduced by ML-60218, for both of the TLR agonists used (Fig. 5*C*), while secretion of IL-6 and TNF-α was also inhibited (Fig. 5*D*). ML-60218 clearly affected translation, since expression of cytokine mRNAs remained untouched by the treatment (Fig. 5*D*). The deficit in costimulatory molecule expression caused by RNA Pol III inhibition was further evaluated following the activation of primary OT2 T cells with ovalbumin peptide (323 to 339)-loaded DCs (Ova-DCs). CellTrace Violet was used to follow T cell proliferation after priming with control or ML-60218–treated DCs. As expected from the reduced expression of both surface CD86 and CD40, OT2 proliferation was strongly reduced when stimulation was provided by RNA Pol III-inhibited Ova-DCs, irrespective of their activation by either LPS or Poly I:C (Fig. 5*E*). This inability to prime naïve T cells observed in the ML-60218–treated DCs, was coincident with a lack of $CD4^+$ T regulatory cell induction, here visualized by the expression the transcription factor Foxp3 in OT2 T cells after activation with control Ova-DCs (Fig. 5*E*). Pol III activity and tRNA gene expression are therefore necessary for DCs to acquire their unique immune-stimulatory capacity in response to TLR agonists.

Discussion

Activated phagocytes or rapidly dividing T cells have important metabolic demands and show strong requirements for energy production and macromolecule biosynthesis (21). Translation is a key step in regulating gene expression and one of the most energy consuming processes in the cell. It is thus predictable that metabolism and protein synthesis should be coordinated by common signaling pathways (30). We have shown that LPS stimulation has a profound impact on the intensity and quality of translation in DCs both in vitro and in vivo (5). This enhancement in protein synthesis is controlled downstream of TLR4 by the PI3K/AKT/mTOR signal transduction pathway and is necessary for cytokine production, as well as the up-regulation of surface costimulatory molecules and MHC class II. We report here that casein kinase 2 activity parallels and potentially synergizes with the AKT/mTOR axis to achieve protein synthesis up-regulation and full DC activation.

CK2 has been described as a stress-activated protein kinase, potentially involved in mRNA translation control (31). Several translation factors are directly phosphorylated by CK2, including subunits of eukaryotic initiation factors eIF3 and eIF5 (32, 33). This impact on protein synthesis, together with the physical

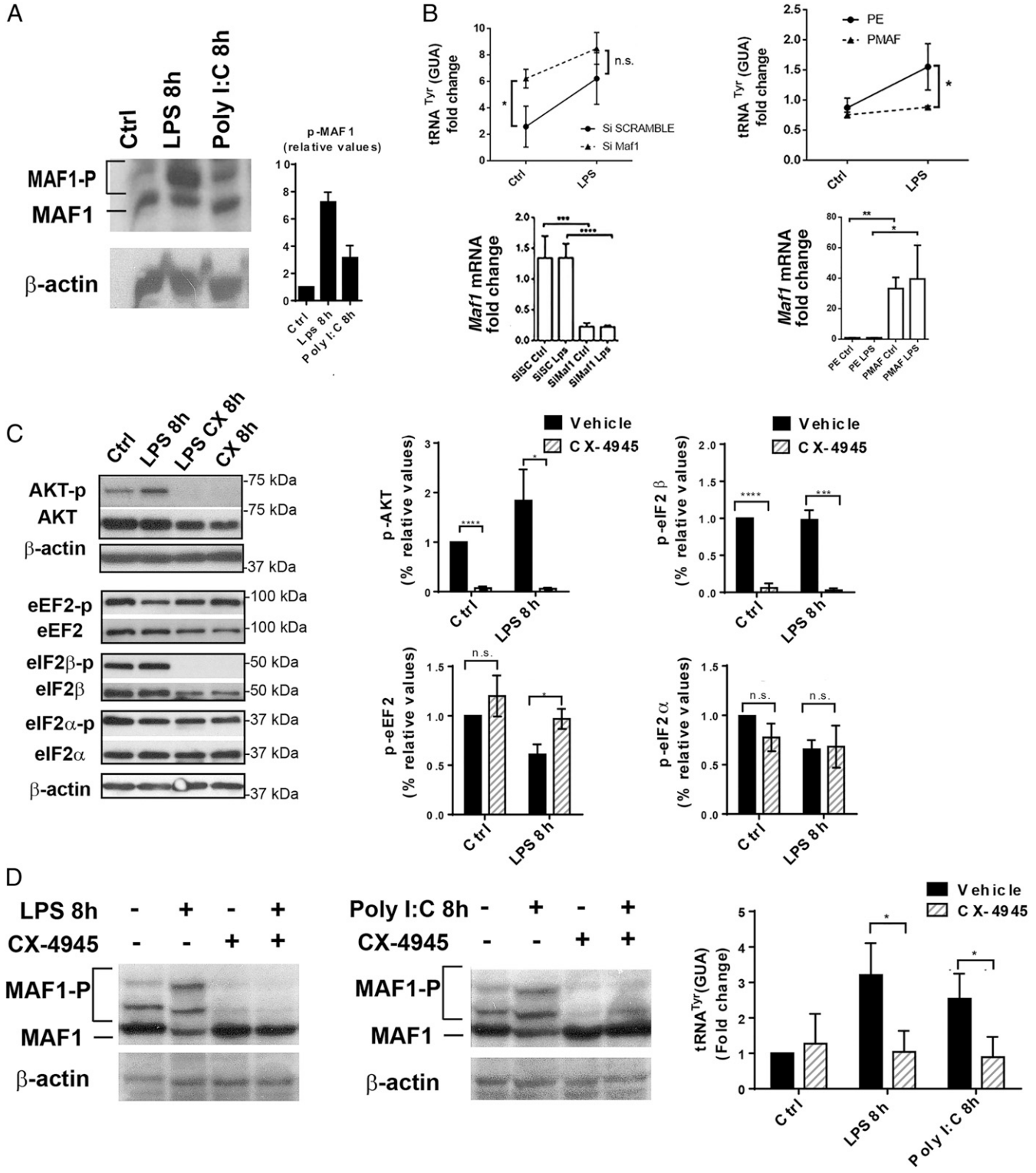

Fig. 3. *MAF1*-dependent Pol III activity is controlled by CK2. (*A*) MAF1 phosphorylation in DCs stimulated with LPS and Poly I:C was analyzed by Phos-Tag immunoblotting; β-actin serves as control. Quantification is shown on the *Right*. (*B*) *Maf1* silencing in DCs (Maf1 KD) and LPS activation for 4 h. Scrambled siRNA (SC) serves as control. *Maf1* overexpression in DCs (PMAF) compared to control transfected with empty vector (PE). $tRNA^{Tyr}$ (GUA) and *Maf1* mRNA levels were analyzed by RT-qPCR. Data are mean ± SD ($n = 3$). (*C*) LPS-activated DCs treated or not with CK2 inhibitor CX-4945 were subjected to immunoblotting. Levels of p-AKT, total AKT, p-eEF2, total eEF2, p-eIF2β, total eIF2β, p-eIF2α, and total eIF2α were analyzed. All data (mean ± SD) are representative of $n = 3$ independent experiments; quantification is shown on the *Right*. (*D*) Phos-Tag immunoblotting for P-MAF1 in DCs stimulated with LPS, Poly I:C, and treated with CX-4945 for 8 h; β-actin is used as control. Levels of $tRNA^{Tyr}$ (GUA) were measured by RT-qPCR. Data are mean ± SD ($n = 3$). In *B*–*D* n.s., nonsignificant results; $^{*}P < 0.05$, $^{**}P < 0.01$, $^{***}P < 0.001$, and $^{****}P < 0.0001$ were obtained by unpaired Student's *t* test.

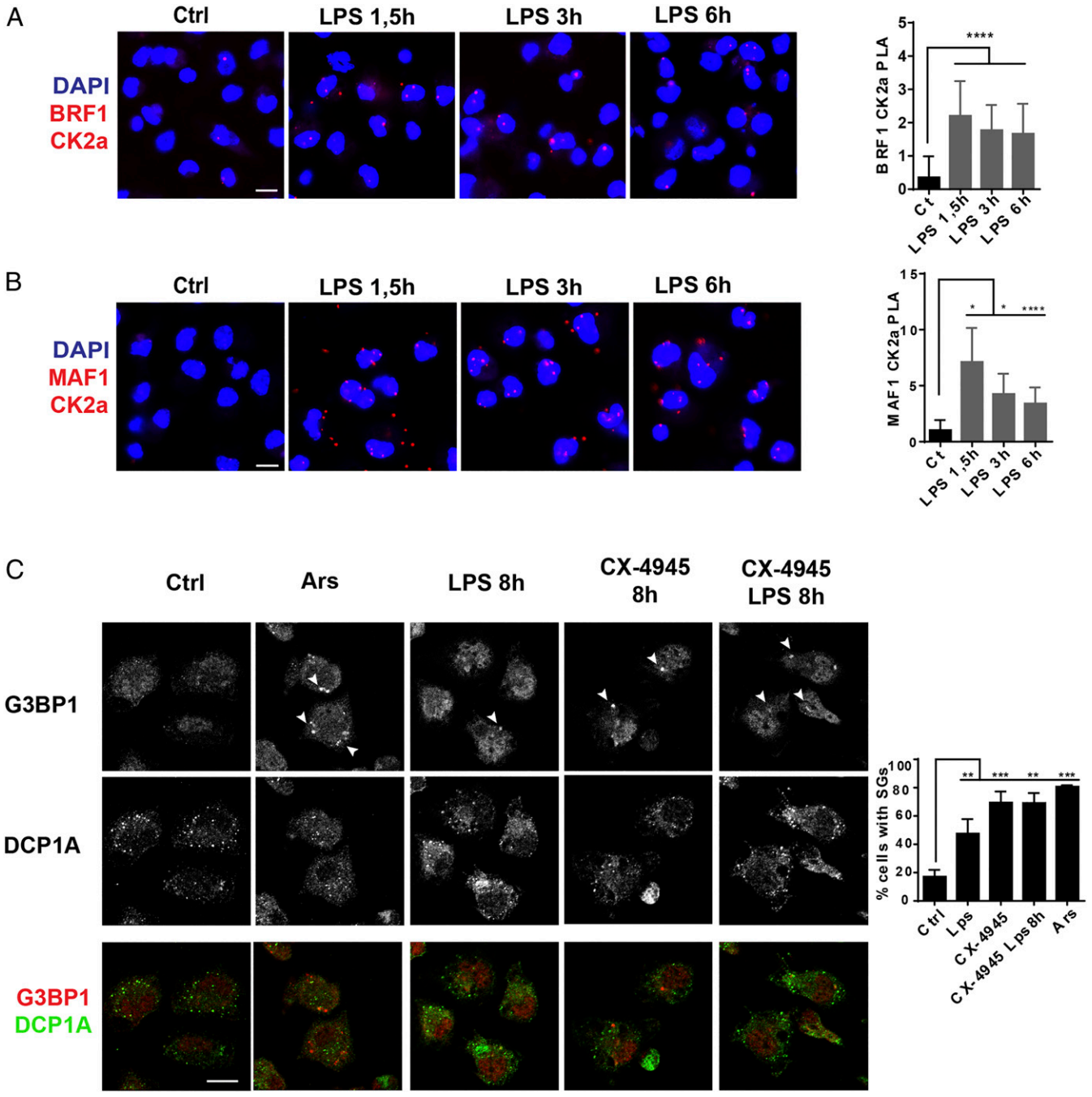

Fig. 4. CK2 is a regulator of Pol III activity. (*A* and *B*) iPLA of DCs stimulated with LPS for indicated time and stained for BRF1 and CK2a (*A*), or MAF1 and CK2a (*B*). (*C*) Confocal microscopy for G3BP1 and DCP1A of DCs stimulated with LPS and treated with CX-4945. Cells treated 30 min with arsenite were used as positive reference. G3BP1-positive SGs are indicated by arrowheads. (Scale bar, 10 μm.) All Images are representative of $n = 3$ independent experiments. Quantification (mean ± SD) is shown on the *Right*. *$P < 0.05$, **$P < 0.01$, ***$P < 0.001$, and ****$P < 0.0001$ were obtained with multiple comparison with Holm–Sidak correction.

interaction, direct phosphorylation, and cross-regulation of AKT by CK2, partially explains the correlation between CK2 activity and elevated rates of cell proliferation (34). Upon TLR stimulation by MAMPs, CK2 plays a key role in coordinating RNA Pol III-dependent tRNA transcription and raises protein synthesis activity to the level required to achieve DC maturation. Direct targeting by CK2 of the nuclear repressor MAF1, in synergy with mTORC1 activity, is required for these processes, thus confirming that in mammalian cells, similar mechanisms exist as those seen in yeast switching from respiratory conditions to fermentative growth (26). Basal CK2 activity is necessary to maintain AKT, MAF1, and NF-κβ phosphorylation in steady-state DCs, suggesting that CK2 inhibitors could have strong antiinflammatory properties by targeting several key pathways for DC homeostasis and activation.

One of the major consequences of CK2-dependent Pol III activation associated with TLR signaling is the up-regulation of tRNA expression. We demonstrated that enhanced Pol III activity is necessary to maintain ad hoc protein synthesis levels in LPS-activated DCs, but not in resting cells. Pol III inhibition

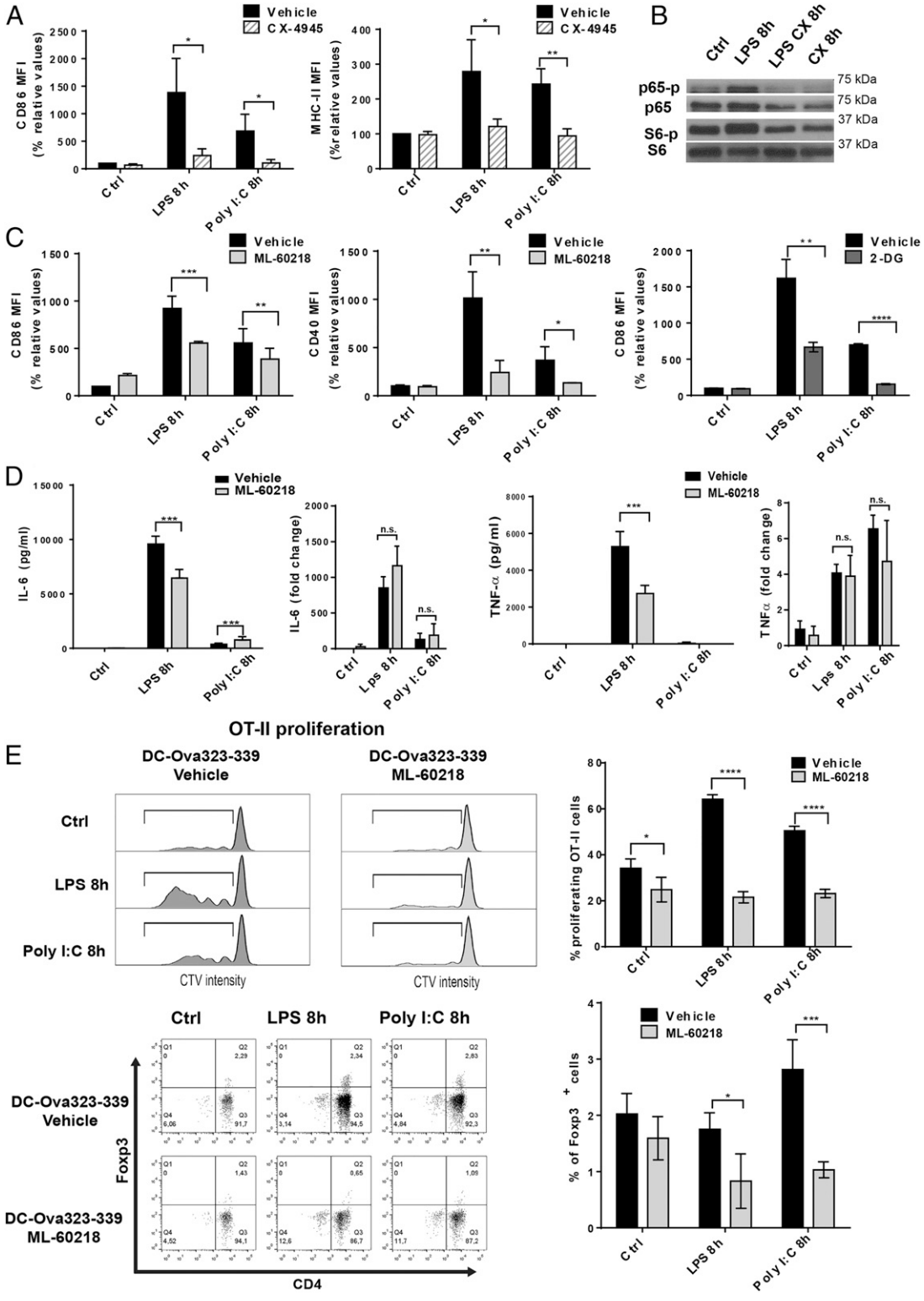

Fig. 5. Pol III activity is required for DC activation and T cell priming. (*A*) DCs stimulated with LPS, Poly I:C, and treated with CX-4945. Surface up-regulation of costimulatory molecules CD86 and MHCII was measured by flow cytometry and is presented as mean fluorescence intensity (MFI). (*B*) DCs activated with LPS, treated with CK2 inhibitor CX-4945 for 8 h, and processed for immunoblotting. Analysis of p-p65, p65, p-S6, and S6 levels. (*C*) DCs stimulated with LPS, Poly I:C, and treated with the Pol III inhibitor ML-60218 for 8 h. Surface up-regulation of costimulatory molecules CD86 and CD40 was measured by flow cytometry and is presented as MFI. DCs were also stimulated with LPS, Poly I:C, and treated with 2-DG for 8 h, and surface CD86 levels were analyzed by flow cytometry. Data are mean ± SD (n = 3). $^{*}P < 0.05$, $^{**}P < 0.01$, $^{***}P < 0.001$ by unpaired Student's t test. (*D*) The concentrations of secreted IL-6 and TNF-α were measured by ELISA. IL-6 and TNF-α mRNA levels were quantified by RT-qPCR. Data are mean ± SD (n = 3). $^{***}P < 0.001$ by unpaired Student's t test. (*E*) OT-II proliferation assay. DCs stimulated with LPS, Poly I:C, and treated with ML-60218 for 8 h and loaded with the OVA 323 to 339 peptides. DCs were incubated with CellTrace Violet (CVT)-labeled OT-II/Rag-$2^{-/-}$ T cells for 4 d and analyzed by flow cytometry for CTV dilution and Foxp3 expression. Quantification of the percentage of proliferating OT-II cells and $Foxp3^{+}$ cells are shown on the *Right*. Data are mean ± SD (n = 3). n.s., nonsignificant results; $^{*}P < 0.05$, $^{**}P < 0.01$, $^{***}P < 0.001$, $^{****}P < 0.0001$ by unpaired Student's t test.

causes accumulation of mRNAs in SGs and prevents the up-regulation of surface molecules, like CD86 or CD40, necessary for mature DCs to prime naïve T cells. tRNA synthesis and Pol III transcription are therefore necessary to achieve functional DC activation, to the same extent as the glycolytic switch observed upon TLR stimulation. DC activation by MAMPs is almost systematically associated with type-I IFN production and exposure, which accelerates the process of DC maturation and acquisition of T cell priming competence. Type-I IFN also up-regulates many nucleic acid modifying and degrading enzymes that globally function to counteract viral replication in infected cells (18, 35), with the consequences of promoting cytosolic nucleic acid degradation and also potentially tRNA and rRNA decay. In activated DCs, this processing could be detrimental to maintain robust protein synthesis and could interfere globally with the activation process. Thus, enhanced Pol III activity in type-I IFN-exposed DCs is required to adapt the translation machinery and allow neosynthesis of molecules required for naïve T cell priming. Replacement of the tRNA pool could also have qualitative consequences on the efficiency of translation of specific mRNAs and introduce an additional layer of complexity to the gene expression regulatory program governing DC activation (36). The CK2/MAF1/Pol III signaling axis represents a further pathway that could be pharmacologically harnessed to control immunity and inflammation in pathological situations.

ACKNOWLEDGMENTS. The P.P./E.G. laboratory is "Equipe de la Fondation de la Recherche Médicale" sponsored by the grant DEQ20140329536. The project was also supported by grants from l'Agence Nationale de la Recherche (ANR), ANR-FCT 12-ISV3-0002-01, A*MIDEX project "CSI" (ANR-11-IDEX-0001-02), DCBIOL Labex ANR-11-LABEX-0043, INFORM Labex ANR-11-LABEX-0054, funded by the "Investissements d'Avenir" French government program. The research was also supported by the Ilídio Pinho foundation, Fundação para a Ciência e a Tecnologia, and Programa Operacional Competitividade e Internacionalização Compete2020 (Fundo Europeu de Desenvolvimento Regional [FEDER]) references PTDC/IMI-IMU/3615/2014, POCI-01-0145-FEDER-016768, and POCI-01-0145-FEDER-030882. We acknowledge financial support from ANR-10-INBS-04-01 France Bio Imaging and the ImagImm of the Centre d'Immunologie de Marseille-Luminy imaging and cytometry core facility.

1. M. Dalod, R. Chelbi, B. Malissen, T. Lawrence, Dendritic cell maturation: Functional specialization through signaling specificity and transcriptional programming. *EMBO J.* **33**, 1104–1116 (2014).
2. S. Akira, S. Uematsu, O. Takeuchi, Pathogen recognition and innate immunity. *Cell* **124**, 783–801 (2006).
3. R. M. Steinman, Dendritic cells: Understanding immunogenicity. *Eur. J. Immunol.* **37** (suppl. 1), S53–S60 (2007).
4. I. Mellman, Dendritic cells: Master regulators of the immune response. *Cancer Immunol. Res.* **1**, 145–149 (2013).
5. H. Lelouard *et al*., Regulation of translation is required for dendritic cell function and survival during activation. *J. Cell Biol.* **179**, 1427–1439 (2007).
6. A. Pantel *et al*., Direct type I IFN but not MDA5/TLR3 activation of dendritic cells is required for maturation and metabolic shift to glycolysis after poly IC stimulation. *PLoS Biol.* **12**, e1001759 (2014).
7. I. M. Willis, R. D. Moir, Signaling to and from the RNA polymerase III transcription and processing machinery. *Annu. Rev. Biochem.* **87**, 75–100 (2018).
8. E. P. Geiduschek, G. A. Kassavetis, The RNA polymerase III transcription apparatus. *J. Mol. Biol.* **310**, 1–26 (2001).
9. G. A. Kassavetis, G. A. Letts, E. P. Geiduschek, The RNA polymerase III transcription initiation factor TFIIIB participates in two steps of promoter opening. *EMBO J.* **20**, 2823–2834 (2001).
10. P. Cabart, J. Lee, I. M. Willis, Facilitated recycling protects human RNA polymerase III from repression by Maf1 in vitro. *J. Biol. Chem.* **283**, 36108–36117 (2008).
11. R. Upadhya, J. Lee, I. M. Willis, Maf1 is an essential mediator of diverse signals that repress RNA polymerase III transcription. *Mol. Cell* **10**, 1489–1494 (2002).
12. P. Ivanov, N. Kedersha, P. Anderson, Stress granules and processing bodies in translational control. *Cold Spring Harb. Perspect. Biol.* **11**, a032813 (2018).
13. G. Clavarino *et al*., Protein phosphatase 1 subunit Ppp1r15a/GADD34 regulates cytokine production in polyinosinic:polycytidylic acid-stimulated dendritic cells. *Proc. Natl. Acad. Sci. U.S.A.* **109**, 3006–3011 (2012).
14. M. Reverendo *et al*., TRNA mutations that affect decoding fidelity deregulate development and the proteostasis network in zebrafish. *RNA Biol.* **11**, 1199–1213 (2014).
15. S. Kirchner *et al*., Alteration of protein function by a silent polymorphism linked to tRNA abundance. *PLoS Biol.* **15**, e2000779 (2017).
16. I. Avcilar-Kucukgoze *et al*., Discharging tRNAs: A tug of war between translation and detoxification in Escherichia coli. *Nucleic Acids Res.* **44**, 8324–8334 (2016).
17. L. Wu *et al*., Novel small-molecule inhibitors of RNA polymerase III. *Eukaryot. Cell* **2**, 256–264 (2003).
18. B. Ogunjimi *et al*., Inborn errors in RNA polymerase III underlie severe varicella zoster virus infections. *J. Clin. Invest.* **127**, 3543–3556 (2017).
19. S. Kimura, M. K. Waldor, The RNA degradosome promotes tRNA quality control through clearance of hypomodified tRNA. *Proc. Natl. Acad. Sci. U.S.A.* **116**, 1394–1403 (2019).
20. B. Everts *et al*., TLR-driven early glycolytic reprogramming via the kinases TBK1-IKKε supports the anabolic demands of dendritic cell activation. *Nat. Immunol.* **15**, 323–332 (2014).
21. L. A. O'Neill, E. J. Pearce, Immunometabolism governs dendritic cell and macrophage function. *J. Exp. Med.* **213**, 15–23 (2016).
22. U. Sheth, R. Parker, Decapping and decay of messenger RNA occur in cytoplasmic processing bodies. *Science* **300**, 805–808 (2003).
23. C. Sidrauski, A. M. McGeachy, N. T. Ingolia, P. Walter, The small molecule ISRIB reverses the effects of eIF2α phosphorylation on translation and stress granule assembly. *eLife* **4**, e05033 (2015).
24. A. Aulas *et al*., Stress-specific differences in assembly and composition of stress granules and related foci. *J. Cell Sci.* **130**, 927–937 (2017).
25. M. Boguta, Why are tRNAs overproduced in the absence of Maf1, a negative regulator of RNAP III, not fully functional? *PLoS Genet.* **11**, e1005743 (2015).
26. D. Graczyk *et al*., Casein kinase II-mediated phosphorylation of general repressor Maf1 triggers RNA polymerase III activation. *Proc. Natl. Acad. Sci. U.S.A.* **108**, 4926–4931 (2011).
27. M. Haddach *et al*., Synthesis and SAR of inhibitors of protein kinase CK2: Novel tricyclic quinoline analogs. *Bioorg. Med. Chem. Lett* **22**, 45–48 (2012).
28. F. Buontempo *et al*., Therapeutic targeting of CK2 in acute and chronic leukemias. *Leukemia* **32**, 1–10 (2018).
29. S. A. Gibson, E. N. Benveniste, Protein kinase CK2: An emerging regulator of immunity. *Trends Immunol.* **39**, 82–85 (2018).
30. R. J. Argüello, C. Rodriguez Rodrigues, E. Gatti, P. Pierre, Protein synthesis regulation, a pillar of strength for innate immunity? *Curr. Opin. Immunol.* **32**, 28–35 (2015).
31. M. Sayed, S. O. Kim, B. S. Salh, O. G. Issinger, S. L. Pelech, Stress-induced activation of protein kinase CK2 by direct interaction with p38 mitogen-activated protein kinase. *J. Biol. Chem.* **275**, 16569–16573 (2000).
32. G. Arrigoni *et al*., Mass spectrometry analysis of a protein kinase CK2beta subunit interactome isolated from mouse brain by affinity chromatography. *J. Proteome Res.* **7**, 990–1000 (2008).
33. F. Meggio, L. A. Pinna, One-thousand-and-one substrates of protein kinase CK2? *FASEB J.* **17**, 349–368 (2003).
34. M. Ruzzene, J. Bertacchini, A. Toker, S. Marmiroli, Cross-talk between the CK2 and AKT signaling pathways in cancer. *Adv. Biol. Regul.* **64**, 1–8 (2017).
35. K. Malathi, B. Dong, M. Gale, Jr, R. H. Silverman, Small self-RNA generated by RNase L amplifies antiviral innate immunity. *Nature* **448**, 816–819 (2007).
36. Z. R. Newman, J. M. Young, N. T. Ingolia, G. M. Barton, Differences in codon bias and GC content contribute to the balanced expression of TLR7 and TLR9. *Proc. Natl. Acad. Sci. U.S.A.* **113**, E1362–E1371 (2016).

PNAS
www.pnas.org

Supplementary Information for

Polymerase III transcription is necessary for T cell priming by dendritic cells

Marisa Reverendo, Rafael J. Argüello, Christine Polte, Jan Valečka, Voahirana Camosseto, Nathalie Auphan-Anezin, Zoya Ignatova, Evelina Gatti and Philippe Pierre

Email: pierre@ciml.univ-mrs.fr

This PDF file includes:

Supplementary Material and Methods
Figs. S1 to S4
Tables S1 to S4

www.pnas.org/cgi/doi/10.1073/pnas.1904396116

Supplemental Material and Methods

Reagents

Reagents and used concentrations were as follows: HMW Poly(I:C) (10 μg/mL)) was from InvivoGen; LPS (Escherichia coli O55:B5) (100 ng/ml), Rapamycin (100 nM) and Sodium Arsenite (500 μM, 30min) were from Sigma-Aldrich. RNA Polymerase III Inhibitor ML-60218 (50μM) was from Merck. CX-4945 (Silmitasertib)(10 μM) was from Abcam. ISRIB (750 nM) was a gift from Peter Walter, UCSF, San Francisco.

Mice

Wild-type (WT) female C57BL/6 mice were purchased from Janvier, France; Ifnar1-/- mice (B6.129S2-Ifnar1^{tm1agt}) were a kind gift of Elena Tomasello (Dalod Lab, CIML); animals were maintained in the animal facility of Centre d'Immunologie de Marseille-Luminy (CIML). OT-II mice (12) on a RAG-2 deficient background were kept in CIPHE and were a kind gift of Sandrine Henri (Malissen Lab, CIML). Animals were kept under specific pathogen–free conditions accredited by the French Ministry of Agriculture to perform experiments on live mice. This study was carried out in strict accordance with the recommendations in the Guide for the Care and Use of Laboratory Animals of the French Ministry of Agriculture and of the European Union. All experiments were approved by the Comité d'éthique de Marseille and the Direction Départementale des Services Vétérinaires des Bouches du Rhône (approval number A13-543). All efforts were made to minimize animal suffering.

Molecular Biology and gene expression analysis

4×10^6 BM-DCs were transfected with 4 ug of origene pCMV6 mouse Maf1 plasmid and pCMV6 empty plasmid using the Amaxa Mouse Dendritic Cell Nucleofector™ Kit following the provider´s instructions. Cells were activated 12 h post transfection and analysed. FlexiTube siRNA targeting *Maf1* and FlexiTube siRNA scramble as control (QIAGEN) were used for RNA silencing experiments. 4×10^6 BM-DCs were transfected with 1 μg of siRNA using the Amaxa Mouse Dendritic Cell Nucleofector™ Kit. Cells were activated 16 h post transfection and analysed. Total RNA was isolated using Trizol® (Invitrogen) and the Direct-zol™ kit (Zymo Research). cDNA was prepared with random hexamers and SuperScript III reverse transcriptase (Invitrogen). Real-time qPCR analysis was performed using SYBR Green PCR master mix (Takara) with Applied Biosystems PRISM 7700 Sequence Detection System. Primers are listed in Table S1.

Translation intensity measurement - Puromycin labelling

Puromycin labelling for measuring translation levels was done as previously described (Schmidt et al., 2009). Puromycin (Sigma-Aldrich) was added at 12,5µg/ml to the culture medium and the cells were incubated for 15 min at 37°C and 5% CO2. After puromycin incorporation the cells were harvested, washed in PBS and processed with Cytofix/Cytoperm buffer (BD Biosciences), stained with the anti-puromycin antibody (12D10) directly coupled with Alexa Fluor 488, and diluted in Perm/Wash buffer (BD Biosciences). Samples were acquired on a FACS Canto II (BD Biosciences), and data were analysed using FlowJo (Tree Star).

Immunofluorescence

Cells were harvested and dropped on a 12-mm coverslip covered with alcian blue. The coverslips were then incubated for 10 min at 37°C and fixed with 3,7% paraformaldehyde for 10min at room temperature. Cells were permeabilized with 0,1% Triton X-100 in 5% FCS PBS with 100 mM glycine, for 15 min at room temperature and stained over night at 4ºC with indicated primary antibodies, MAF1 (Abgent), G3BP1 and DCP1A (Santa Cruz). Coverslips were mounted using Prolong Gold and images taken with a laser-scanning confocal microscope (LSM 780; Carl Zeiss MicroImaging) using a 63× objective and accompanying imaging software. Nuclear and cytosolic quantification was performed using the isolateCells.ijm Image J pluggin developed by Jan Valečka (CIML and Labex INFORM).

Confocal immunofluorescence microscopy combined with fluorescent mRNA *in situ* hybridization (FISH) or immuno-proximity ligation assay.

Cells on coverslips were fixed with 3.7% formaldehyde for 15 min, then permeabilized in 70% EtOH overnight and blocked with 5% bovine serum albumin (Sigma) containing ribonucleoside vanadyl complex (2 mM). Cells were stained for G3BP1 and RNase inhibitor (Rnasin, Promega) was added to the staining buffer. After this, cells were washed with 10% formamide in 2× SSC. A fluorescent probe (Quasar 570) against CD86 mRNA (Stellaris, Biosearch Technologies) was diluted in hybridization buffer containing dextran sulfate 10 mg/ml and 10% formamide in 2× SSC, according to the manufacturer's instructions. Probe was incubated with cells for 4 h at 37°C. Coverslips were mounted with Prolong Gold containing DAPI (Invitrogen). For immuno-proximity ligation assay (iPLA), cells were layered on a 12-mm coverslip covered with alcian blue. The coverslips were incubated for 10 min at 37°C and fixed with 3,7% paraformaldehyde for 10min at room temperature. iPLAs were done using the Duolink Kit according to the manufacturer’s instructions (Sigma-Aldrich). Specifically, the primary antibodies were: mTOR and CK2a from Santa Cruz and BRF1 was form Abcam. Duolink iPLA Probe anti-rabbit minus and anti-mouse plus were used. Samples were incubated in the ligation solution consisting of Duolink Ligation Stock and Duolink Ligase. Detection of the amplified probe was done with the Duolink Detection Kit Orange. All confocal microscopy images acquisition was performed with an LSM 780 laser-scanning microscope (Carl Zeiss MicroImaging) using a 63× objective.

Microarrays analysis.

tRNA microarrays were performed as previously described (14). Shortly, total RNA (5-10 µg) was extracted from cells at basic conditions using TRIzol® (Invitrogen) which leads to complete deacylation of tRNAs (14). Cy3- or Atto647-labeled stem-loop RNA/DNA oligonucleotide was ligated overnight at 16°C with T4 DNA ligase (NEB) to all deacetylated tRNAs. The tRNAs isolated from sample at the onset of experiment (zero-time point) were labeled with Atto647-labeled stem-loop oligonucleotide, while the samples representing other time points with Cy3-labeled one and hybridized together on one microarray for 16 h at 60°C in. The arrays were normalized to spike-in standards (14) and quantified with in-house python and R scripts.

For gene expression analysis the total RNA was isolated with RNeasy kit (Qiagen). cDNA was synthesized with random hexamers and superscript II reverse transcriptase (Invitrogen). Quantitative real-time PCR analysis was performed with Applied Biosystems PRISM 7700 Sequence Detection System. The list of primers used is included in supplementary table 1. For Affymetrix microarray analysis, GM-CSF DCs were cultured in RPMI supplemented with 5 % FCS, 50µM beta-mercaptoethanol and GM-CSF. Cells differentiated for 6 days were treated for 8h with microbial stimuli and harvested before lysis. Control and Proteus mirabilis treated DCs were incubated with the bacteriostatic chloramphenicol to avoid bacterial growth. Guanabenz was used at 50 µM. Hybridization to arrays (Affymetrix GeneChip Mouse Gene 1.0ST) and image scanning were performed according to the Affymetrix Expression Analysis Technical Manual. Gene Expression microarray raw data were normalized using limmaGUI software (R/Bioconductor, Boston, MA, USA). Data are deposited in the GEO repository (GSE90831).

T cell proliferation

T cell proliferation assays were performed as described in (16). Briefly, the spleens and lymph nodes of OT-II *Rag-2*$^{-/-}$ mice were used, cells were isolated using a CD4 untouched Dynabeads® kit (Invitrogen). Purified OT-II Rag-2−/− T cells were labelled with CellTrace ™ Violet (Invitrogen). A total of 3 × 10^3 DCs were cocultured with 2 × 10^4 CTV-labeled OT-II *Rag-2*$^{-/-}$ T cells in 150 µL in the presence of ovalbumin (323-339) peptide (0.03 µg/mL). After 4 days of culture, proliferation (a loss of CTV staining) and Foxp3 expression were measured by flow cytometry. Foxp3 expression levels were analysed using the Foxp3 staining set (eBioscience) following the manufacturer's protocol.

Statistical analysis

Statistical analysis was performed using GraphPad Prism Software. * P<0.5, ** P<0.01, *** P< 0.001, ****P<0.0001. Mainly unpaired Student's *t*-test was used. Additionally, multiple comparisons analysis with the Holm-Sidak correction was used when comparing multiple treatments and covariance analysis was performed on the tRNA microarray data.

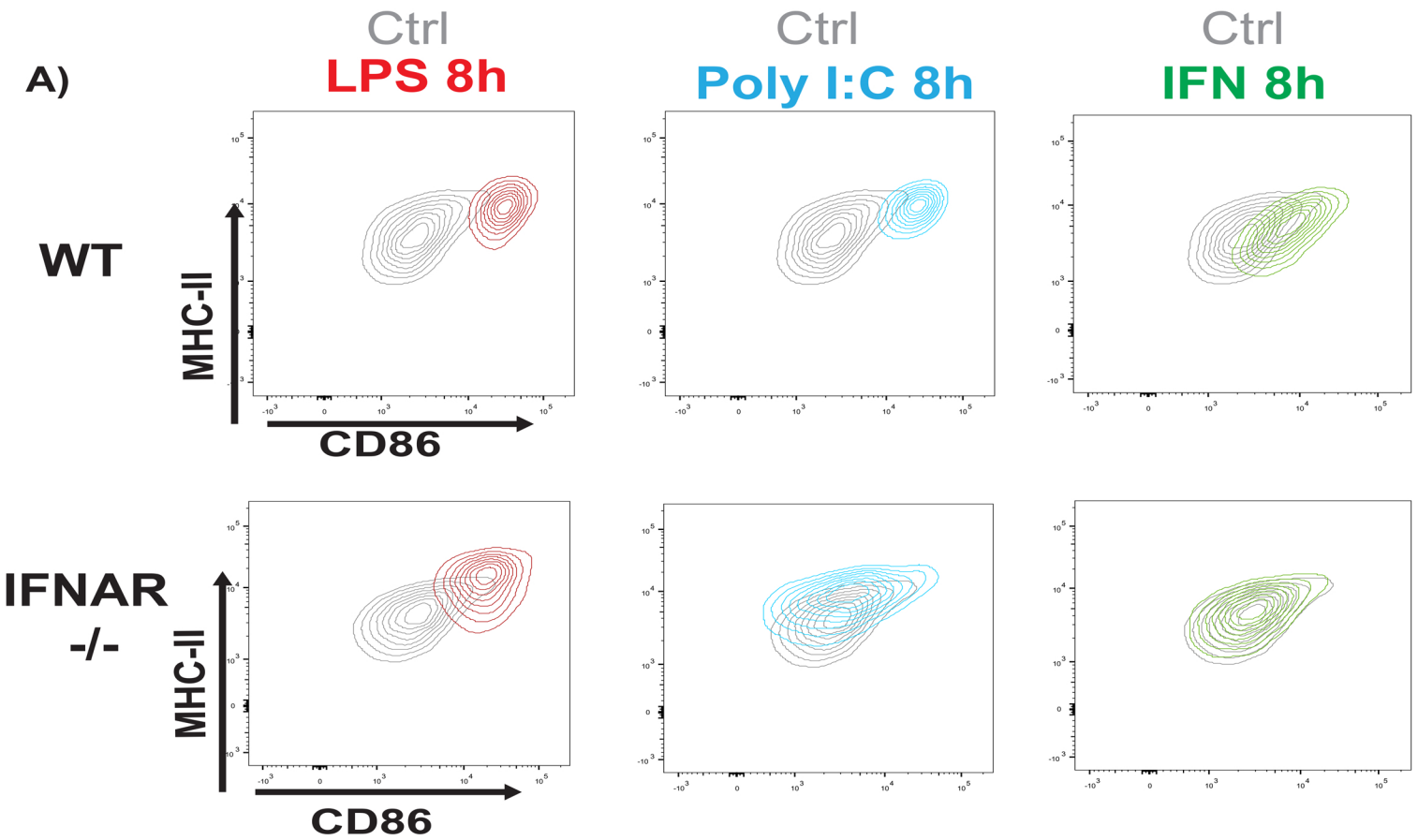

Supplementary Figure S1. DC maturation is delayed in absence of IFNAR. WT and IFNAR -/- DCs were stimulated with LPS, Poly I:C and Interferon β for 8h. Surface upregulation of co-stimulatory molecules CD86 and MHCII was measured by flow cytometry. Data are representative of three independent biological experiments.

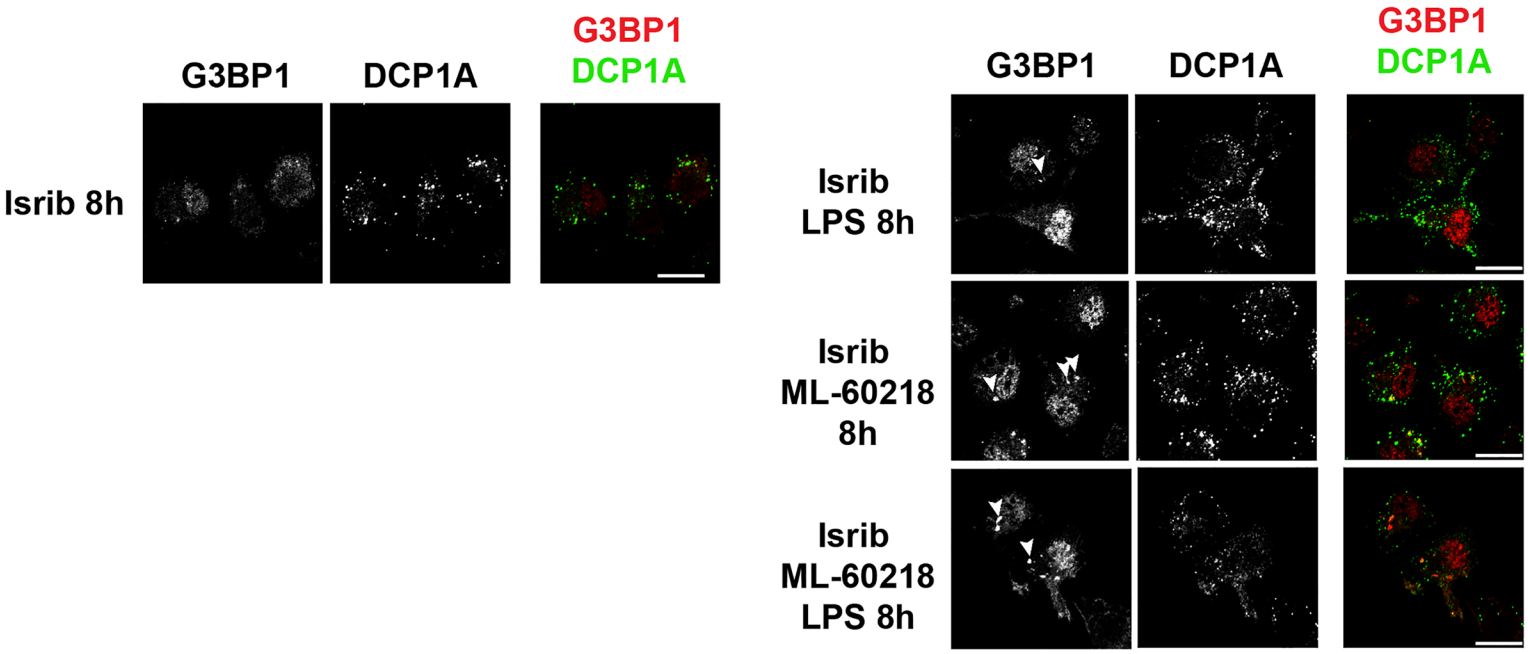

Supplementary Figure S2. SG formation is not inhibited in presence of ISRIB. Immunofluorescence microscopy for G3BP1 and DCP1A of DCs stimulated with LPS, Poly I:C and treated with ML-60218 and ISRIB for 8h. Data is representative of three independent experiments G3BP1-positive SGs are marked with arrowheads. Scale bar, 10 μm.

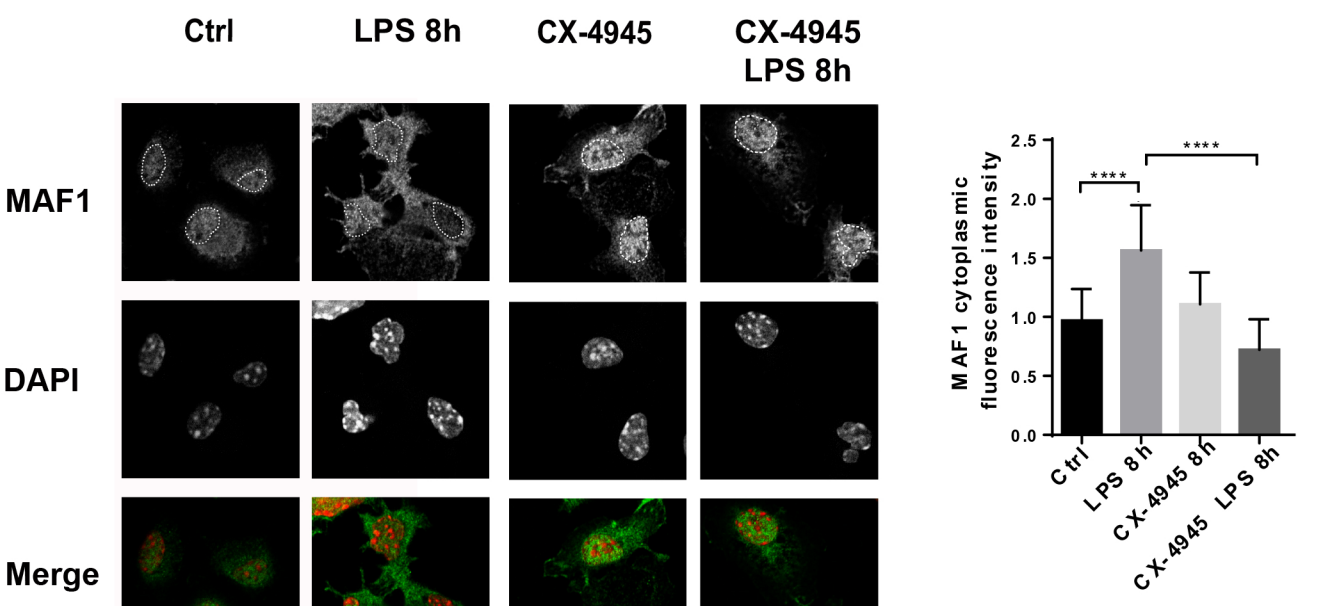

Supplementary Figure S3. CK2 inhibition prevents MAF1 export from the nucleus of LPS activated DCs. Immunofluorescence microscopy for MAF1 in DCs stimulated with LPS and treated with CX-4945 for 8h. Images are representative of three independent experiments. Nuclei were counterstained with DAPI and nuclear area is marked with a dashed line. Scale bar, 10 μm. Quantification is shown as MAF1 relative fluorescence intensity in the cytosol (n>25) ****P < 0.0001.

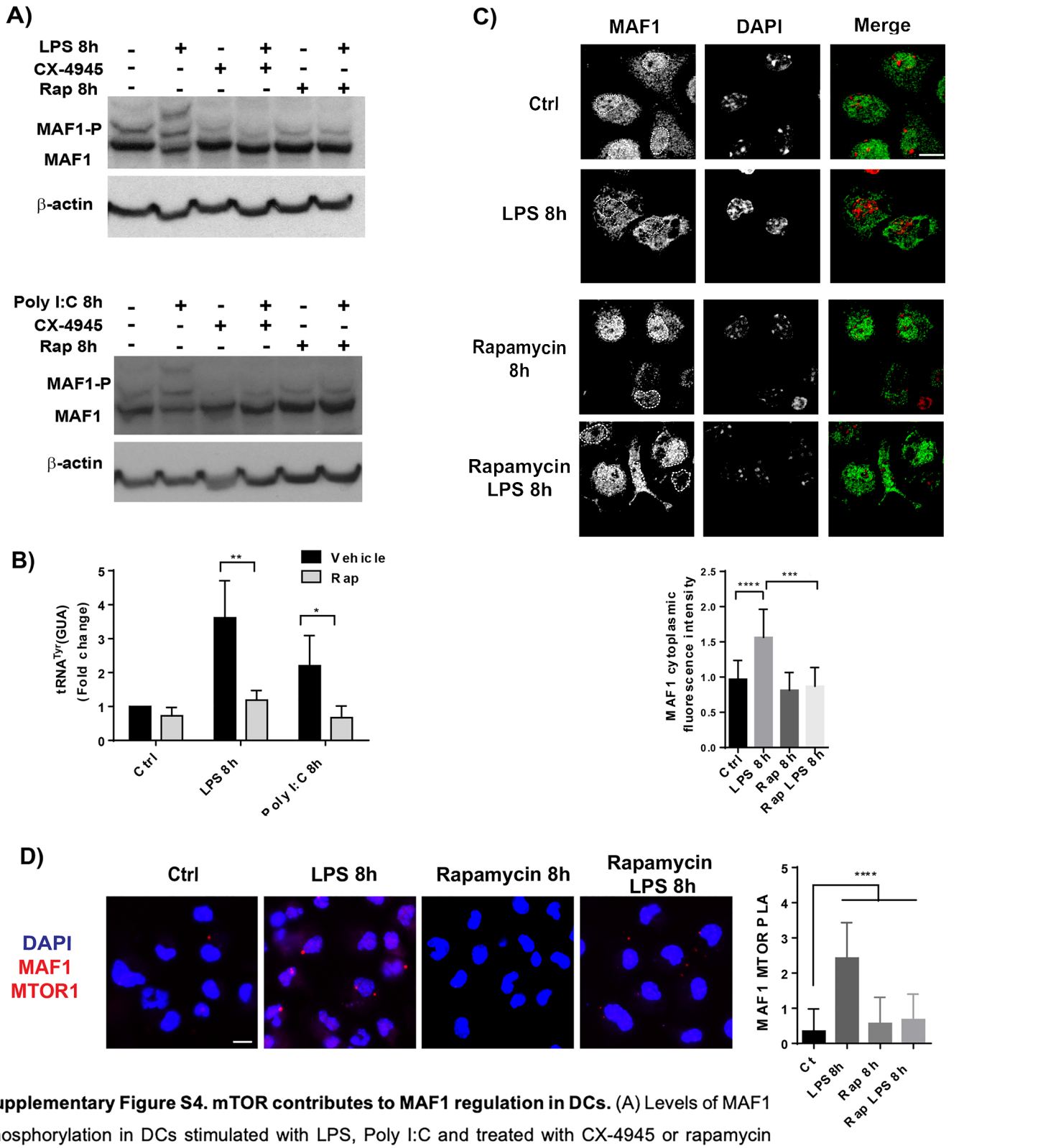

Supplementary Figure S4. mTOR contributes to MAF1 regulation in DCs. (A) Levels of MAF1 phosphorylation in DCs stimulated with LPS, Poly I:C and treated with CX-4945 or rapamycin (rap) for 8h analysed using Phos-tag™ immunoblotting, β-actin served as loading control. Data is representative of three independent experiments with similar results. (B) Levels of tRNA^{Tyr} (GUA) measured by RT-qPCR. Data are mean ± SD (n = 3 independent samples). *P < 0.05, **P < 0.01 by unpaired student's t-test. (C) Immunofluorescence microscopy for MAF1 in DCs stimulated with LPS and treated with Rapamycin for 8h. Images are representative of three independent experiments. Nuclei were counterstained with DAPI and nuclear area is marked with a dashed line. Scale bar, 10 μm. Quantification is shown as MAF1 relative fluorescence intensity in the cytosol (n>25), ***P < 0.001, ****P < 0.0001. D) Immunofluorescence proximity ligation assay (iPLA) of DCs stimulated with LPS for indicated times and stained for MAF1 and mTOR. Confocal images are representative of three independent experiments. Quantification of the iPLA foci per cell is shown on the right of the panel. Data are mean ± SD (n = 3). ****P < 0.0001 by multiple comparison with Holm–Sidak correction.

Supplementary Table 1

Primer sequences used for RT-qPCR.

Target	**Sequence**
POLR3CFw	GGTAAGAGGAGGAGATCATCTG
POLR3CRev	GGTTGACTTGCCAATAAATCCC
Maf1Fw	TTGCCAAGCCAACCCCACACT
Maf1Rev	TGCTTGCTCATCGAGGGAGGT
IL6Fw	AGTCCTTCCTACCCCAATTTCC
IL6Rev	GTCTTGGTCTGCTGCCACTCC
TnfαFw	GATATTGTTGCGAGGGCTGCC
TnfαRev	GAGGATTGCTATCACACTATTC
Internal control	CAATTGCAGATGAGATGGATCA
RPS16Fw	ATTTGCTGGTGTGGATATTCG
RPS16Rev	CTTGGAGGCTTCATCCACATA

Supplementary Table 2

tRNAs expression levels in WT and IFNAR -/- DCs stimulated with LPS for 8h. tRNAs were quantified by tRNA-tailored microarrays. tRNAs are represented by the anticodon and cognate amino acid. Meti-CAU denotes initiator tRNA pairing to AUG start codon. Data are means of two biological replicates which were highly reproducible similar 0.76, 0.85, 0.88 and 0.87 (Kolmogorov-Smirnov test) for WT LPS 4h, WT LPS 8h, IFNAR-/- LPS 4h and IFNAR-/- 8h, respectively. Bold indicates a considerably higher expression of the tRNA in IFNAR-/- DC stimulated for 8h with LPS than in WT cells.

tRNA	WT LPS 4h	WT LPS 8h	IFNAR-/- LPS 4h	IFNAR-/- LPS 8h
Arg-ICG	1,61	0,83	0,72	1,65
Arg-C/UCG	1,56	0,80	0,67	1,61
Arg-CCU	**1,55**	**0,95**	**0,99**	**2,01**
Arg-UCU	1,67	0,88	0,83	1,50
His-GUG	1,40	1,06	1,19	0,96
Lys-CUU	1,38	0,93	0,81	0,79
Lys-UUU1	**1,44**	**0,87**	**0,92**	**3,38**
Lys-UUU2	1,33	1,04	0,81	0,73
Lys-UUU3	1,57	0,95	1,15	1,42
Asp-GUC	1,13	0,75	0,59	0,70
Glu-UUC	1,30	0,79	0,78	1,25
Glu-C/UUC	1,22	0,79	0,83	1,12
Asn-GUU	1,40	0,83	0,80	1,07
Cys-UGU/C	1,35	0,98	0,94	1,50
Gln-C/UUU	**1,30**	**1,01**	**0,99**	**2,01**
Ser-CGA	1,23	1,04	0,89	0,89
Ser-A/G/UGA	1,30	1,06	0,80	0,69
Ser-GCU	1,15	0,97	0,82	0,72
Thr-A/CGU	1,37	1,16	1,04	1,15
Thr-UGU	1,46	1,05	0,99	1,44
Thr-CGU	1,91	1,47	0,91	1,32
Ala-A/C/UGC	**1,31**	**1,10**	**0,98**	**2,76**
Gly-G/CCC	1,54	1,17	0,58	1,57
Gly-UCC	1,06	1,09	1,10	1,35
Ile-IAU	1,32	1,35	0,92	1,70
Ile-UAU	**2,13**	**1,07**	**0,94**	**3,34**
Leu-A/UAG	**1,54**	**1,05**	**0,92**	**2,31**
Leu-CAG	**1,45**	**0,94**	**0,89**	**2,14**
Leu-CAA	1,43	1,06	0,99	1,43
Leu-UAA1	1,76	0,95	0,78	1,88
Leu-UAA2	**1,26**	**0,76**	**0,94**	**3,52**
Meti-CAU	1,02	0,90	1,13	1,18
Met-CAU	1,32	1,11	0,95	1,59
Phe-GAA	1,25	1,18	0,99	1,35
Pro-A/C/UGG	1,39	0,85	0,71	0,66
Sec-UCA2	1,18	1,04	0,85	0,64
Trp-CCA	1,33	1,02	0,99	1,39
Tyr-GUA	1,13	0,89	0,78	0,71
Val-mAC	1,08	1,06	0,92	0,89
Val-UAC	1,50	1,24	0,97	1,04

Supplementary Table 3

Covariance analysis of the tRNAs expression levels in DCs stimulated with LPS for 4 and 8h. The values for WT (A) and IFNAR -/- (B) DCs stimulated for 4 and 8h were compared. tRNAs are represented by the anticodon and cognate amino acid. Meti-CAU denotes initiator tRNA pairing to AUG start codon.